# Well-Defined P III -Terminated Polymers from Phosphorylated Carbodithioate RAFT Agents

Andrii Karpus, Simon Harrisson, Rinaldo Poli, Stéphane Mazières, Eric Manoury, Mathias Destarac

**Well-defined $P^{III}$-terminated polymers from phosphorylated carbodithioate RAFT agents**

Andrii Karpus,[a,b] Simon Harrisson,[c] Rinaldo Poli,[a] Stéphane Mazières,*[b] Eric Manoury*[a] and Mathias Destarac*[b]

*[a] Dr. A. Karpus, Prof. R. Poli, Dr. E. Manoury*

*CNRS, LCC (Laboratoire de Chimie de Coordination),*

*Université de Toulouse, UPS, INPT,*

*205 Route de Narbonne, BP 44099, 31077 Toulouse, France*

*E-mail: eric.manoury@lcc-toulouse.fr*

*[b] Dr. A. Karpus, Dr. S. Mazières, Prof. M. Destarac*

*Laboratoire des IMRCP, Université Paul Sabatier, CNRS UMR 5623*

*118 route de Narbonne 31062 Toulouse, France*

*E-mail: destarac@chimie.ups-tlse.fr*

*[c] Dr. S. Harrisson*

*Laboratoire de Chimie des Polymères Organiques,*

*Université de Bordeaux/ENSCBP/CNRS UMR 5623*

*16 avenue Pey Berland 33607 Pessac, France*

**ORCID**

Andrii Karpus: 0000-0002-5760-3086

Simon Harrisson: 0000-0001-6267-2599

Rinaldo Poli: 0000-0002-5220-2515

Stephane Mazières: 0000-0003-1266-4659

Eric Manoury: 0000-0001-7991-8890

Mathias Destarac: 0000-0002-9718-2239

## Graphical abstract

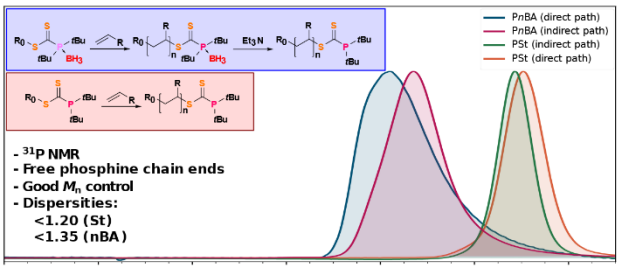


## Abstract

Five S-alkyl di-*tert*-butylphosphorylated carbodithioates, Z-C(S)SR, were studied as chain transfer agents (CTAs) in the RAFT polymerization of vinyl monomers. These phosphorus-containing CTAs involve new $P^{III}$ and $P^{V}$ moieties in the Z group (phosphine-borane or free phosphine). Two of them, with an S-bonded 1-methoxycarbonylethyl group as leaving group, have not previously been described. The CTAs with a $P^{V}$ Z group provide good control over the polymerization of styrene (St) and *n*-butyl acrylate (*n*BA). Molar masses are close to theoretical values and dispersities are consistently low during polymerization. The monitoring of polymerization by $^{31}P$ NMR spectroscopy supports the controlled character and the integrity of the polymer chain ends. Conversely, they inhibit the polymerization of the less-activated monomer vinyl acetate (VAc). The reactivity of the CTAs with a $P^{III}$ Z group mainly depends on the reaction medium, and their performance for St, *n*BA and VAc was surprising and unexpected. Theoretical calculations were carried out in order to rationalize their behavior. Finally, an innovative strategy was developed to obtain well-controlled polymers with free phosphine ω-chain ends.

## Introduction

Reversible addition-fragmentation chain transfer (RAFT)[1,2] polymerization is a widely-applied tool for macromolecular design. The essential component of this type of reversible-deactivation radical polymerization[1] is a chain transfer agent (CTA) with the general formula Z-C(S)S-$R_0$. The CTA efficiency is determined by the reactivity of the C=S double bond, which is strongly affected by the nature of Z-group[3,4] and by the lability of the S-$R_0$ bond[5] in the initiation step. Therefore, for the polymerization of a particular monomer, it is of great importance to select a CTA with appropriate Z and $R_0$ groups in order to moderate the reactivity of the carbodithioate group, with Z playing a key role in the stability of the intermediate radical. The most successful families of RAFT agents[6,7] are dithioesters[8,9] (Z = alkyl or aryl), dithiocarbamates[10,11] (Z = $NR_2$), dithiocarbonates or xanthates[3,12] (Z = OR) and trithiocarbonates[8,13] (Z = SR). Several hundred of these compounds have been developed and their efficiency in RAFT polymerization has been systematically studied. Nevertheless, each CTA is suitable to control the polymerization of only a narrow range of monomers except for isolated cases like *N*-methyl-*N*-(4-pyridinyl)[14,15] and *N*-aryl-*N*-(4-pyridinyl)[16] dithiocarbamate switchable RAFT agents or CTAs of intermediate reactivity such as *O*-alkyl xanthates[17,18] or pyrazole-based dithiocarbamates.[19,20] A few examples of more "exotic" CTAs based on Z-groups involving other elements including heteroelements have also been described: fluorine[21], selenium[22–24], tin[25,26] or phosphorus.[27–33] The introduction of heteroelements with nuclei of half-integer spin allows the use of NMR spectroscopy to study the CTA consumption, kinetics and mechanisms at the early stages of the polymerization process, as well as for the characterization of the ω-chain end functionality of the obtained polymers.[23,24,27–30]

Phosphorus-containing CTAs (P-RAFT) offer a possible reactivity modulation by coordination of the P atom to a metal (for $P^{III}$ agents, Z = $P^{III}(R)_2 \rightarrow Mt/L$)[30,31] or by varying the

electron-withdrawing strength of the phosphorus atom substituents (for $P^V$ agents, e.g. Z = $P(E)R_2$, E = O, S).[29,33] Despite simple and effective syntheses, P-RAFT CTAs are still rather scarce. Nevertheless, interest in such compounds has grown because of the good control obtained for more-activated monomers such as styrene (St) and *n*-butyl acrylate (*n*BA). However, to the best of our knowledge RAFT polymerizations with a free (*i.e.* not coordinated) $P^{III}$ as a function in the CTA Z group have not been described. Indeed, a comparison of the reactivity of either $P^{III}$ and $P^V$, or free and coordinated $P^{III}$ CTA derivatives in polymerization would significantly aid the fundamental understanding of the Z-group impact. A potential switch between $P^V$ and $P^{III}$ would lead to an increase in the efficiency spectrum of these agents from more-activated monomers to less-activated monomers. In addition, a free $P^{III}$ ω-chain end-functionality for the obtained polymers may open new applications via its ligand properties, for instance coordination to metal cations or to metal nanoparticles.[34]

We have recently reported the simple and effective gram-scale synthesis of various S-(1-phenylethyl)(di-*tert*-butylphosphorylated)carbodithioates with different substituents on phosphorus (**1**-**3** in Figure 1), explored their spectral properties and described simple chemical transformations between members of the series.[35] In particular, we have obtained for the first time thiocarbonylthio compounds with phosphine-borane (**1**) or free phosphine (**3**) as Z groups. In this contribution, we describe the reactivity of these phosphorus-containing RAFT agents, as well as two new related compounds, in the RAFT polymerization of monomers with different reactivity and propose methods for the preparation of free phosphine-terminated polymers.

## Results and discussion

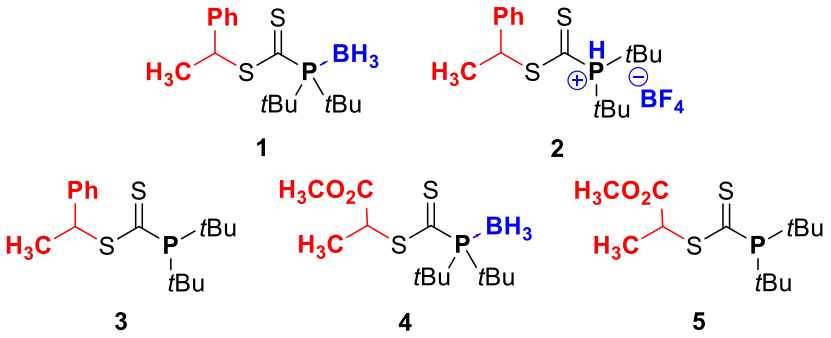


Figure 1. $P^{III}$ - $P^{V}$ CTA derivatives evaluated in RAFT polymerization.

The synthesis of the new CTAs **4** and **5** (Figure 1), containing an S-bonded 1-methoxycarbonylethyl group (acrylate-type radical) as $R_0$, was similar to that previously described for the 1-phenylethyl derivatives **1** and **3**, using methyl 2-bromopropionate as electrophile in the alkylation step instead of 1-bromo-ethylbenzene (see Scheme 1 and experimental part).[35]

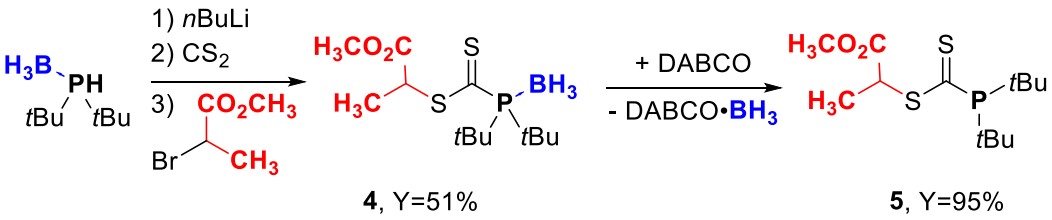


Scheme 1. Synthesis of **4** and **5**.

The efficiency of the P-RAFT agents **1**-**4** was evaluated in the polymerization of *n*BA and St (Scheme 2). CTA **5** was used as a model for polyacrylate-$P^{III}$ chain end in our $^{31}P$ NMR investigations (*vide infra*). All polymerizations reported in Figures 2-5 and Table S1 were carried out in sealed glass tubes at 60°C with azobisisobutyronitrile (AIBN) as thermal initiator and toluene as solvent.

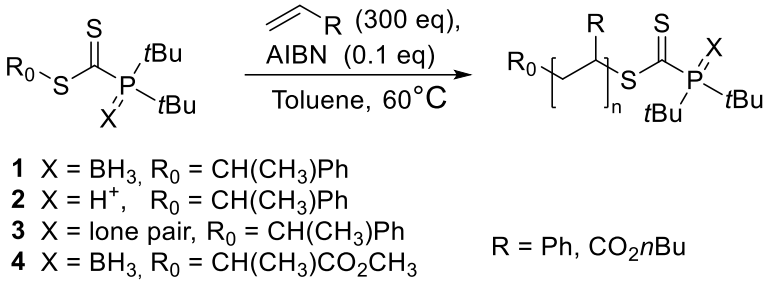


Scheme 2. A general representation of P-RAFT mediated polymerization of St and *n*BA in the presence of CTAs **1**-**4**.

*Polymerization of n-butyl acrylate.* Linear semi-logarithmic plots (Figure 2) were observed in the early stages of the *n*BA polymerizations in the presence of compounds **1**, **3** and **4**, corresponding to pseudo-first-order kinetics with downward deviation from linearity at higher reaction times, which is due to initiator decay. The apparent rate constants ($k_p^{app}=k_p[P^\circ]$) vary as follows: **1** ~ **4** > **3**.

The $BH_3$-derivative **1** and its homologue **4** (differing by the $R_0$ group) afford a good level of control, with $M_n$ close to the targeted one and present moderate dispersities (Đ = 1.25-1.59 for **1**, entries 1-4 of Table S1 and Đ = 1.25-1.49 for **4,** entries 19-24, SEC-RI chromatograms in Figure S13 for **1** and in Figure S15 for **4**) which tend to decrease during the first half of the polymerization and then slightly increase mainly due to the increasing fraction of AIBN-derived chains (Figure 3). Interesting information can be extracted from the $^{31}P$ NMR monitoring. The continuous disappearance of the broadened peaks at 69-70 ppm, corresponding to the phosphorus linked to the $BH_3$ unit (Figures S2 (**1**) and S6 (**4**)) and the observed bleaching of the intensively pink-colored initial solution with time may be due to a gradual thermal degradation of the dormant chain-ends.

With the free phosphine ($P^{III}$) derivative **3,** a poor level of control was observed for the polymerization of *n*BA, with much higher $M_n$ values than expected (Table S1, entries 9-13) and also dispersities ranging between 1.48 and 1.80 (SEC-RI chromatograms, Figure S17).

Additionally, the $^{31}P\{^{1}H\}$ NMR of the reaction mixtures shows the disappearance of the CTA peak at 67.4 ppm after 1 h of polymerization and 2.3% of monomer conversion (Figure S10) with the formation of multiple products. This observation allows us to suppose a non-selective decomposition of the free phosphine thiocarbonylthio chain-end under the polymerization conditions, even though compound **3** was proven to be thermally stable since no changes in the $^{31}P\{^{1}H\}$ NMR spectrum were observed in toluene-$d_8$ at 60°C up to 48 h of heating.[35] The change in color of the polymerization mixture from bright pink to pale orange is another indication of the degradation of the phosphinocarbodithioate group during the polymerization. In addition, when a toluene solution of **3** with 300 eq. of *n*-butyl acrylate was heated at 60°C for 24 h without AIBN, the $^{31}P$ NMR analysis of the resulting solution confirmed the presence of numerous peaks, indicating the instability of **3** under these conditions.

As the ionic CTA **2** was insoluble in toluene, the polymerization of *n*BA with **2** was attempted in acetonitrile at 60°C. No polymer was formed. Instead, a loss of color, the precipitation of insoluble products coming from the decomposition of the functionalized chain-ends, and the disappearance of the $^{31}P\{^{1}H\}$ NMR resonance (Figure S23) were observed after 1 h.

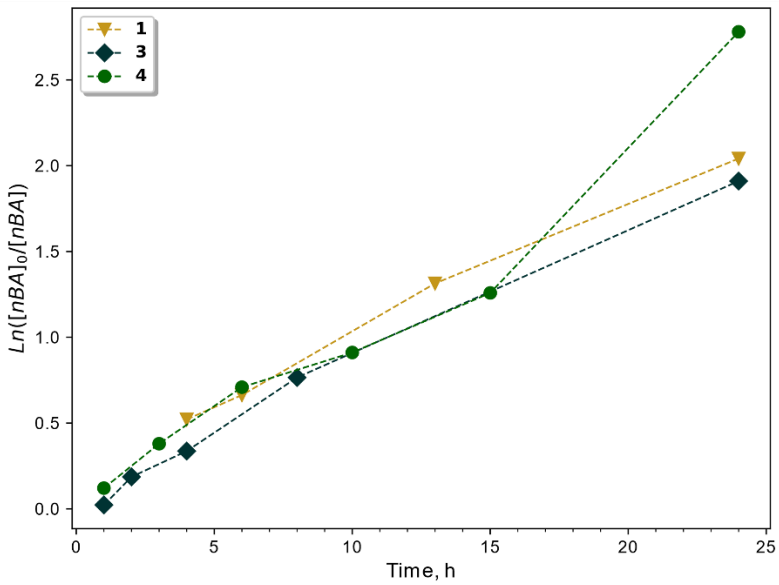


Figure 2. Semi-logarithmic kinetic plot for P-RAFT- mediated polymerization of *n*BA in toluene at 60°C. $[n\text{BA}]_0$ = 5.33 M, $[\text{P-RAFT}]_0$ = 17.8 mM, $[\text{AIBN}]_0$ = 1.78 mM.

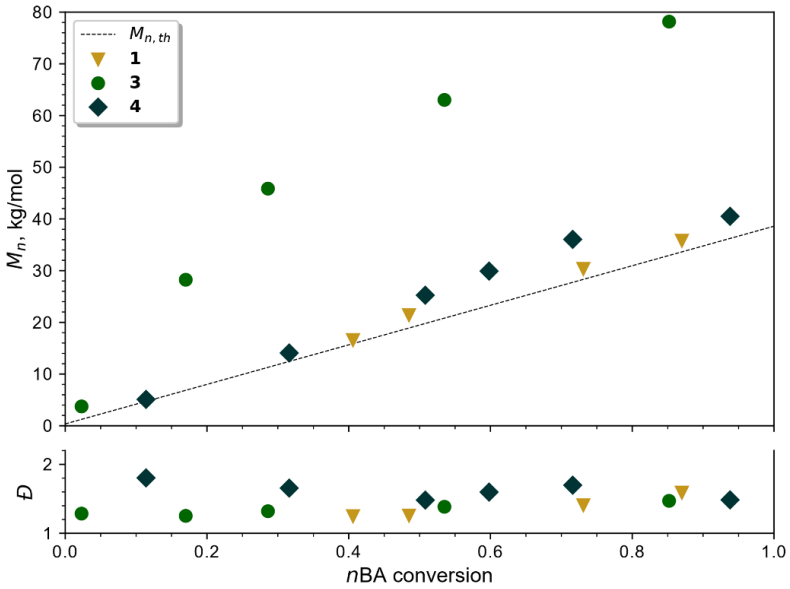


Figure 3. Evolution of $M_n$ and $Đ$ vs monomer conversion in P-RAFT-mediated polymerization of *n*BA at 60°C. Conditions of Figure 2.

*Polymerization of styrene.* As with *n*BA, the reaction of St with CTA **2** led to no polymerization. Compound **2** was immediately and totally decomposed in the reaction medium,

leading to paramagnetic byproducts, incompatible with the NMR analyses. For the other CTAs, the polymerizations were carried out with initial reagent concentration ratio $[St]_0/[CTA]_0$ = 300/1, corresponding to a target theoretical molar mass $M_{n\ th}$ of 31.6 kg $mol^{-1}$. The main conversion-time data and macromolecular characteristics of the obtained polymers are listed in Table S1 and shown in Figures 4 and 5 respectively.

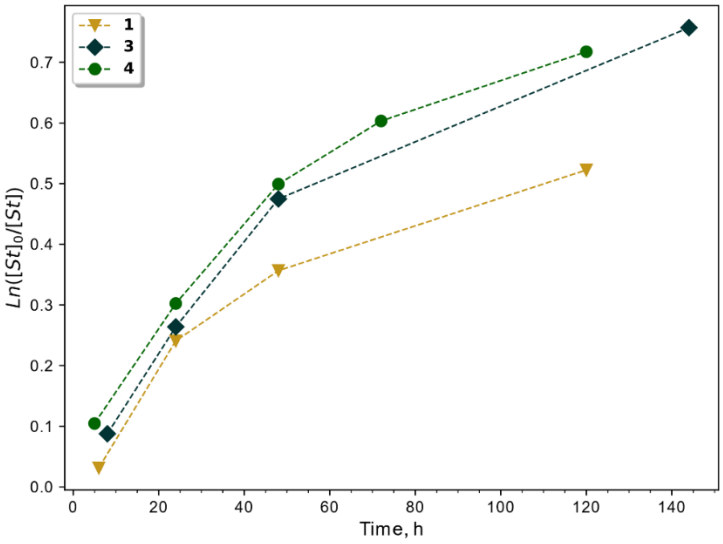


Figure 4. Semi-logarithmic kinetic plot for P-RAFT- mediated polymerization of St in toluene at 60°C. $[St]_0$ = 5.33 M, $[P\text{-}RAFT]_0$ = 17.8 mM, $[AIBN]_0$ = 1.78 mM.

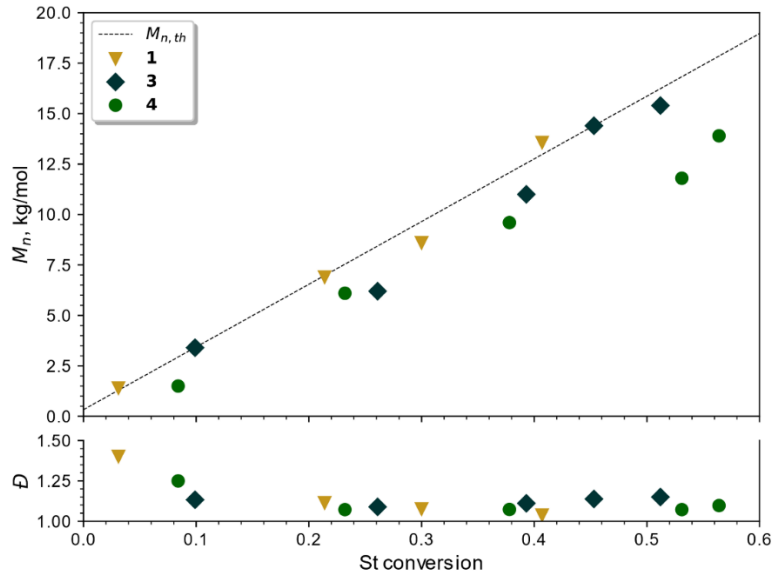


Figure 5. Evolution of $M_n$ and $Đ$ vs monomer conversion in P-RAFT-mediated polymerization of St in toluene at 60°C. Conditions of Figure 4.

Semi-log kinetic plots (Figure 4) in the presence of compounds **1, 3** and **4** revealed a steady-state in macroradical concentration at the beginning of the polymerization (<24 h) and a retardation in the later stages because of the significant reduction in AIBN concentration. Based on the St conversion after 48 h, the apparent rate constants ($k_p^{app}=k_p[P°]$) vary as **4** ~ **3**> **1**.

Both phosphine-borane derivatives **1** and **4** led to a much better control for the polymerization of St than for that of *n*BA, with low dispersities of 1.04 – 1.11 (**1**) and 1.07 – 1.10 (**4**) for the highest conversions (Table S1, **1** entries 6-8, **4** entries 26-29). The SEC analyses also presented the characteristics of well-controlled polymerizations (Figure S14 for **1** and Figure S16 for **4**). The $^{31}P\{^1H\}$ NMR spectra recorded for the polymerization mixtures are given in Figure S4 and Figure S8, respectively. CTA **4** is fully consumed at < 10% conversion, indicating that it has a high transfer constant for St. CTA **1** is fully consumed at ca. 20% conversion. Both **1** and **4** present a similar level of control, with only slightly different dispersities after 120 h of reaction. Contrary to the *n*BA polymerizations (see above), neither

loss of color nor disappearance of the phosphine-borane peak were observed during St polymerizations, which lasted up to 120 h. Thus, the thermal stability of the $BH_3$-CTA derivatives is in accordance with our previous observations[35] and the slow decomposition of the phosphinocarbodithioate end groups during the polymerization of *n*BA may result from a specific reactivity between the phosphinocarbodithioate functionality and *n*BA or the propagating radical, such as the reduction of the *n*BA ester function by borane.

A similar level of control for the polymerization of St was observed with the free phosphine derivative **3**, with dispersities of 1.09 – 1.15 (Table S1, entries 14-18). The results of the SEC analysis are presented in Figure 6. Contrary to the other CTAs of the series, a small peak is visible in the higher molar mass region for the highest reaction times, which is reflected in the slightly higher dispersity values observed (1.15 for **3** compared to 1.10 or lower for **1** and **4**). However, this corresponds to the first example of an efficient RAFT polymerization mediated with a $P^{III}$ phosphino-RAFT agent, thereby allowing the direct preparation of well-controlled PSt samples with free phosphine ω-chain ends.

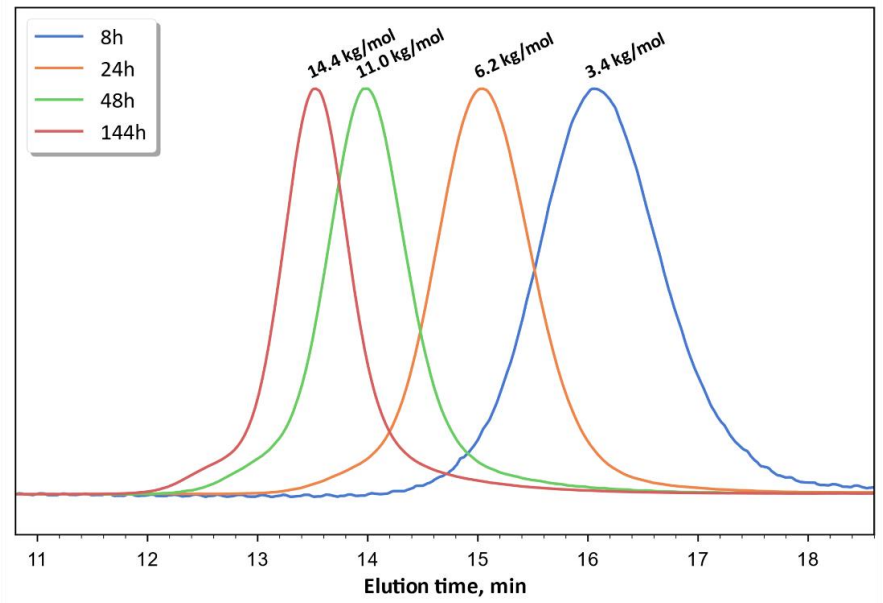

Figure 6. Overlay of the RI-SEC chromatograms of PSt samples obtained in the polymerization mediated by P-RAFT **3**.

To better explore the impact of the electronic difference in the Z-group, a series of St polymerizations were carried out with CTAs **1** and **3** in sealed NMR tubes and stopped at less than 4% monomer conversion (Figures S19-S20). In the case of **3** it was possible to follow the CTA consumption using $^{31}P\{^{1}H\}$ NMR as previously reported, but not for 1 due to broad, overlapping peaks.[32] CTA **3** was completely consumed at monomer conversions < 2% (Table S2, Figure S20). Similar monitoring by 1H NMR spectroscopy, on the other hand, did not allow the same level of precision. This study confirms that 31P{1H} NMR is a powerful tool to quantitatively assess the ability of the P-RAFT agents to transfer to PSt oligoradicals. Analyses performed by SEC at ~1% monomer conversion suggested a more selective formation of oligomers with CTA **3** than for **1** (see figures S21-S22 for the SEC-RI of compounds **1** and **3,** respectively).

*Vinyl acetate.* Compounds **1-3** were not tested as possible CTAs to control the polymerization of vinyl acetate (VAc) due to the very low rate of 1-phenylethyl leaving radical addition to VAc.[36] In contrast, compounds **4** and **5** possess a 1-methoxycarbonylethyl leaving group which adds rapidly and efficiently to VAc.[37,38] Both **4** and **5** completely inhibited the polymerization, similarly to the behavior previously reported for phosphinoyl CTAs.[29,32] This is not surprising for CTA **4** but counter-intuitive for **5**, as this compound, like the xanthates and dithiocarbamates that are efficient RAFT agents for VAc,[11] possesses a lone pair in its Z-group that is available for conjugation with the C=S bond of the thiocarbonylthio function. This result, together with the rather unexpected high reactivity of P(III) RAFT agent **3** in St polymerization led us to consider a theoretical calculation approach.

*Theoretical calculations.* Theoretical calculations were carried out on compound **3** and on related model compounds. In particular we wished to compare related $R_2EC(S)SR_0$ systems (E = N, P), since dithiocarbamates (E = N) are well-known to provide suitable control for the RAFT polymerization of VAc.[11] The first investigated systems, for the purpose of computational efficiency, had the small $CH_3$ as R in the Z group and $R_0$ = $CHMe(O_2CMe)$, which represents a good model of the PVAc chain. The optimizations revealed different configurations at the E atom for these two CTAs: planar for N (sum of the three bond angles = 359.98°) and pyramidalized for P (301.98°), as can be seen in Figure 7. The intermediate of the degenerate exchange process was simulated by the $Me_2EC^{\bullet}[SCHMe(O_2CMe)]_2$ radical. For E = N, the calculated free energy of this intermediate is nearly the same as that of the separate $Me_2EC(S)SCHMe(O_2CMe)$ and $(MeCO_2)CH^{\bullet}Me$ fragments, as expected for an efficient degenerative transfer, assuming that the addition and fragmentation barriers are low. The loss of resonance stabilization for the intermediate in the dithiocarbamate system is evidenced by the slight pyramidalization of the N atom (355.24°) and by the loss of its coplanarity with the $CS_2$ plane. For E = P, on the other hand, the intermediate is more stable than the separate fragments by 10.8 kcal $mol^{-1}$, suggesting a difficult fragmentation process. The P atom pyramidalization is essentially unchanged in the intermediate adduct (303.32°), confirming the absence of resonance stabilization in the starting P-RAFT CTA.

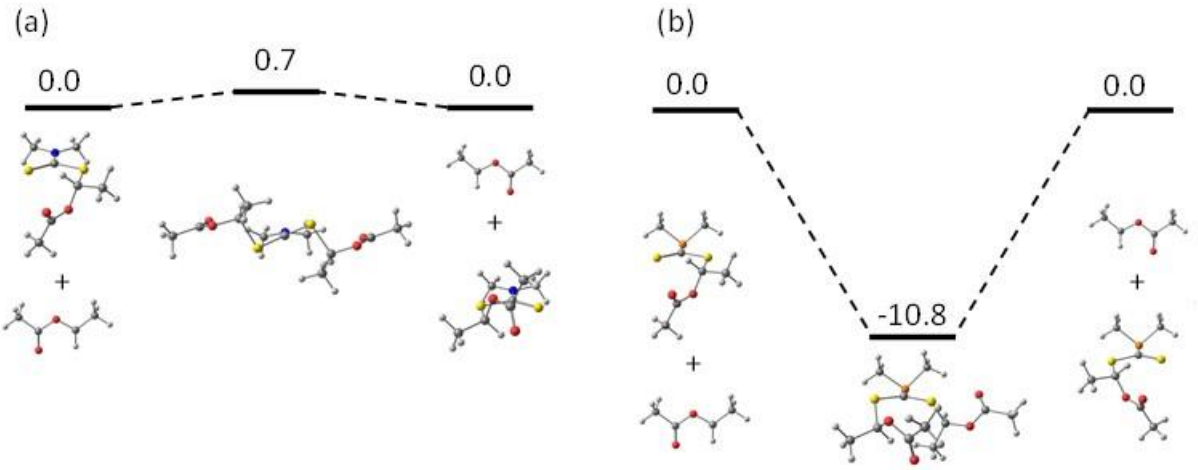


Figure 7. Energy profile (relative $\Delta G$ in kcal $mol^{-1}$) and views of the optimized geometries for the models of the PVAc degenerative exchange with the CTAs $Me_2EC(S)SCHMe(O_2CMe)$: (a) E = N; (b) E = P.

The possible engagement of the P lone pair in a resonance with the $CS_2$ group could be affected by further conjugation and by steric hindrance. These possibilities were probed by optimizing the geometries of the CTAs with R = Ph ($R_0$ = $CHMe(O_2CMe)$) and *t*Bu ($R_0$ = CHMePh), respectively. The resulting geometries are shown in Figure 8. For both systems, the N atom in the dithiocarbamate system has an essentially planar geometry, whereas the P atom in the phosphinocarbodithioate remains markedly pyramidalized. It is remarkable that the large steric encumbrance of the two *t*Bu groups hampers a full conjugation between the $tBu_2N$ and $CS_2$ groups, since the two planes in $tBu_2NC(S)SCHMePh$ are skewed by a dihedral angle of 57°C, but the N atom does not greatly lose its planarity (sum of the bond angles = 350.08°, *vs* 359.99° for the Ph system). On the other hand, the same steric bulk slightly attenuates pyramidalization of the P atom in the phosphinocarbodithioate system, but only from 306.74° for R = Ph to 316.96° for R = *t*Bu.

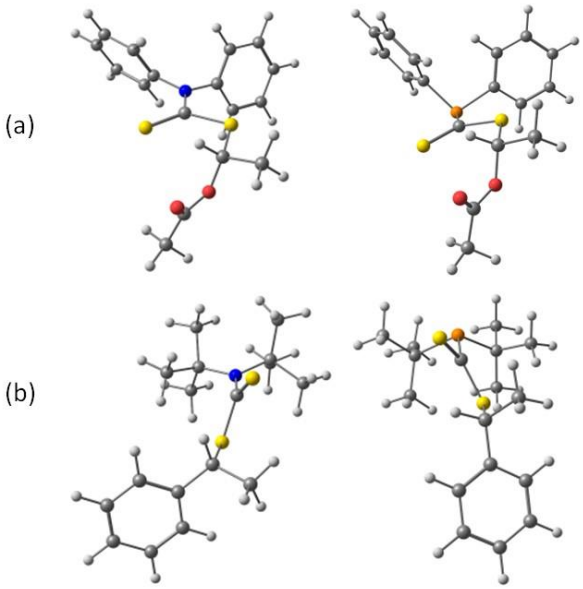


Figure 8. Views of the optimized geometries for (a) $Ph_2EC(S)SCHMe(O_2CMe)$ and (b) $tBu_2EC(S)SCHMe(O_2CMe)$. In both cases, E = N (left) or P (right).

*Well-controlled polymers with $P^{III}$ □-chain ends.* While well-controlled PSt samples can be prepared directly by RAFT polymerization with agent **3** (Scheme 3, top), the same polymer may be also accessible via a two-step polymerization-deboranation procedure with the use of the borane protected RAFT agent **1** (Scheme 3, bottom), followed by treatment of PSt-**1** by triethylamine to remove the borane caps, as previously described for the deboranation of CTA **1**.[35] For the *n*BA polymerization, the $P^{III}$-RAFT CTA **3** showed limitations with no control and NMR evidence for chain-end degradation due to the incompatibility of the $P^{III}$ moiety and *n*BA (see above). To overcome this obstacle in the control of the acrylate monomer polymerization with a free phosphine P-RAFT agent, the two-step polymerization-deboranation procedure was repeated with the use of the borane-protected RAFT agent **4**, which involves an acrylate type leaving group suitable for *n*BA polymerization. This strategy allowed us to achieve the generation of a well-controlled P*n*BA-**4** ($-BH_3$) bearing also $P^{III}$ □-chain ends (Scheme 4).

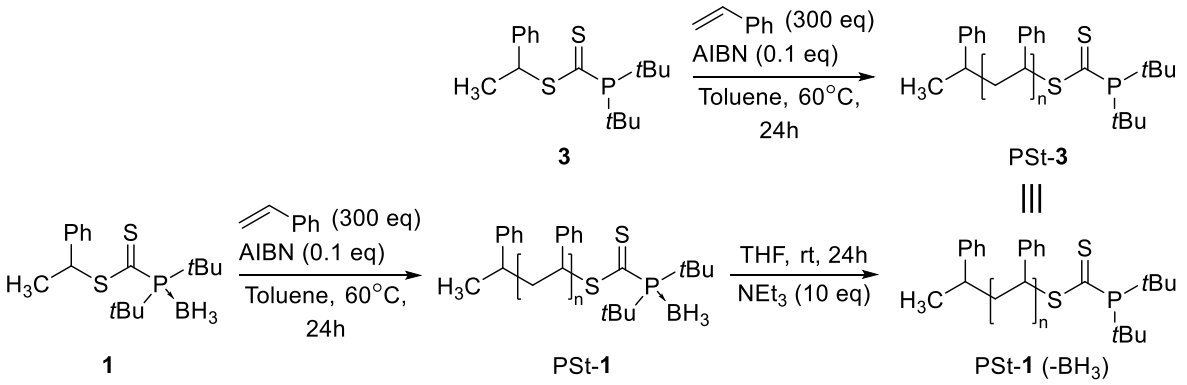


Scheme 3. Preparation of polystyrene with $P^{III}$ ω-chain ends by two pathways: direct application of $P^{III}$-RAFT agent (top), two-step polymerization-deboranation procedure (bottom).

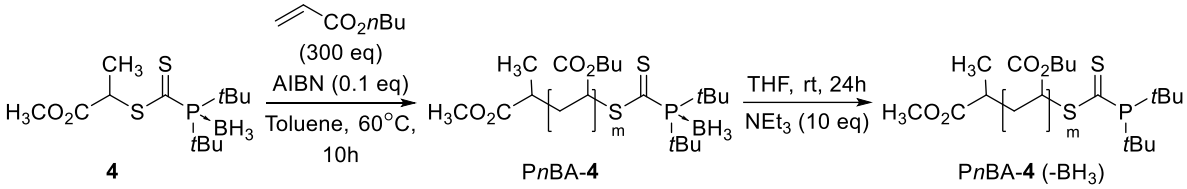


Scheme 4. Preparation of poly(*n*-butyl acrylate) with $P^{III}$ ω-chain ends by a two-step polymerization-deboranation procedure.

The two polymer samples PSt-**1** and P*n*BA-**4** were respectively prepared from CTAs **1** (Scheme 3) and **4** (Scheme 4) in toluene at 60°C. The polymerization was stopped after 24 h for compound **1** and 10 h for compound **4,** yielding PSt-**1** with $M_n$ = 7.1 kg/mol and $Đ$ = 1.06 (Table 1, entry 1) and P*n*BA-**4** with $M_n$ = 28.8 kg/mol and $Đ$ = 1.34 (Table 1, entry 3).

Table 1. Macromolecular characteristics of polymers prior to and after deboranation of the ω-chain ends.

| Entry | Compound | $M_{n,SEC}$, kg/mol[a] | Đ[b] |
|---|---|---|---|
| 1 | PSt-**1** | 7.1 | 1.06 |

| | | | |
|---|---|---|---|
| 2 | PSt-**1** (-$BH_3$) | 7.1 | 1.08 |
| 3 | P*n*BA-**4** | 28.8 | 1.34 |
| 4 | P*n*BA-**4** (-$BH_3$) | 28.4 | 1.35 |

[a] Determined by SEC

[b] $Đ = M_w/M_n$, determined by the SEC.

Subsequent treatment of each product with 10 equivalents of triethylamine at ambient temperature (19°C) for 24 h, followed by concentration under vacuum and removal of all volatile products, gave pure polystyrene samples PSt-**1** (-$BH_3$) with $M_n$ = 7.1 kg/mol and $Đ$ = 1.08 (Table 1, entry 2) and P*n*BA-**4** (-$BH_3$) with $M_n$ = 28.4 kg/mol and $Đ$ = 1.35 (Table 1, entry 4).

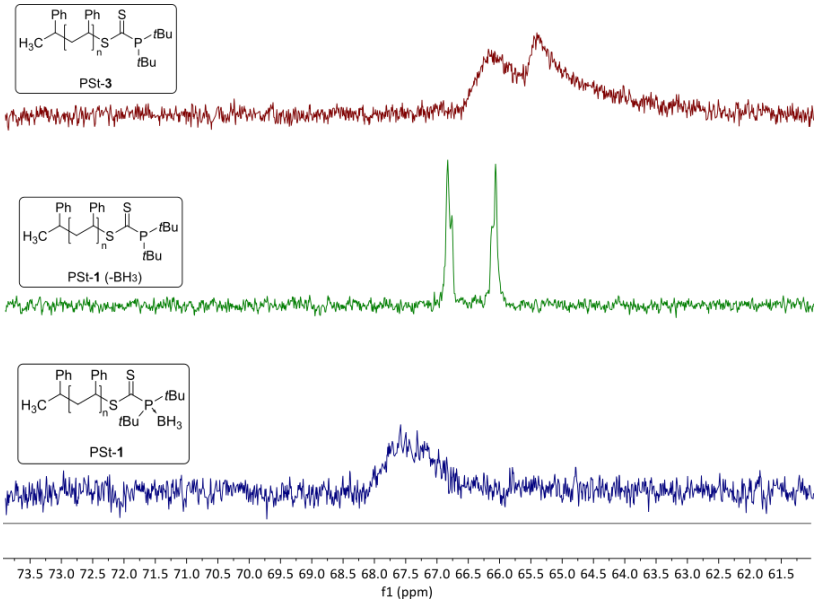


Figure 9: Overlay of the $^{31}P\{^1H\}$ NMR spectra of polystyrene samples prior to (PSt-**1**) and after post-polymerization deboranation (PSt-**1** (-$BH_3$)) of the ω-chain ends. The top trace is the $^{31}P\{^1H\}$ NMR spectrum of the PSt-**3** polymer obtained directly (from Figure S12 after 8 h).

Comparison of the $^{31}P\{^{1}H\}$ NMR spectra of the polymer samples before and after deboranation (PSt: Figure 9; P*n*BA: Figure 10) shows an upfield shift of the ω-chain end resonance along with a change in peak shape (removal of the P-B coupling significantly reduces the linewidth). The presence of two distinct signals for the phosphino chain-ends is not surprising, generally several signals are observed owing to different configurations. In the case of PSt, we can notice that the polymer obtained after deboranation shows resonances at the same chemical shifts as the polymer obtained by direct polymerization from **3**. The difference in the resonance linewidth may be due to different concentrations and purity. As expected for P*n*BA, the resonances of the deboranated polymer are located in the same region as the starting CTA **5**. The SEC-RI chromatograms of the polymer samples prior to (PSt-**1** and P*n*BA-**4**) and after post-polymerization deboranation (PSt-**1** (-$BH_3$) and P*n*BA-**4** (-$BH_3$)) of the ω-chain ends are almost identical, which show the absence of chain coupling during the deboranation process (Figures S31 and S32 respectively).

The direct polymerization of St with a free di-*t*-butylphosphino CTA like **3** or a simple polymerization-deboranation procedure for PSt and P*n*BA via phosphino-borane (P-$BH_3$) containing CTAs like **1** or **4** makes possible preparation of well-controlled polymer samples with free phosphine ω-chain ends by the RAFT process. This makes these polymers ready for complexation with metal cations, metal nanoparticles or other systems and opens a range of new applications.

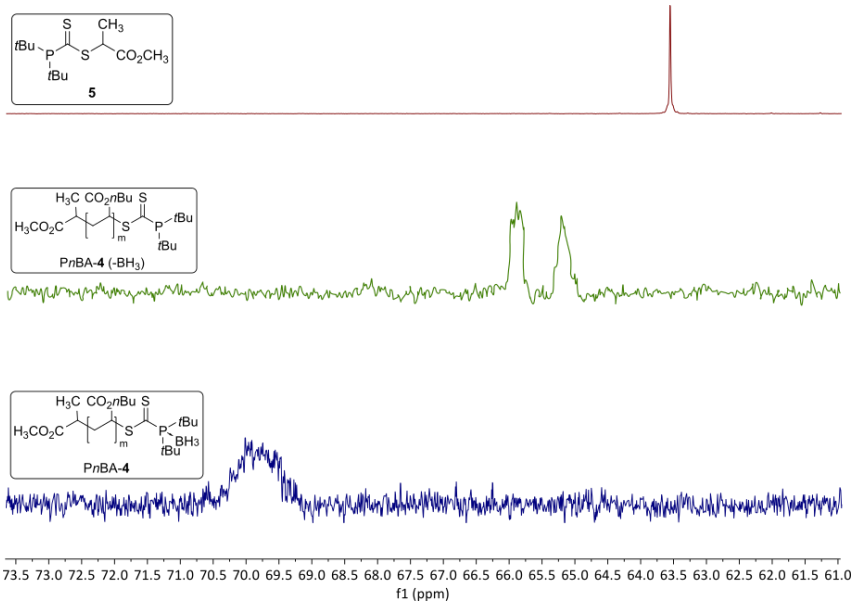


Figure 10: Overlay of $^{31}P\{^{1}H\}$ NMR spectra of poly(*n*-butyl acrylate) samples prior to (P*n*BA-**4**) and after post-polymerization deboranation (P*n*BA-**4** (-$BH_3$)) of the ω-chain ends. Top is the spectrum of CTA **5** alone.

## Conclusions

In the present contribution, we have described investigations on RAFT agents involving various types of phosphorylated functions in the Z-group, including the free phosphine *t*$Bu_2$P-, and their efficiency in the control of the St and *n*BA polymerizations. Extension of the already established synthetic methodology for *t*$Bu_2$P(X)-C(S)$SR_0$ with $R_0$ = CHMePh (X = $BH_3$, **1**; X = nothing, **3**; Figure 1) allowed access to two new phosphinoylcarbodithioate RAFT agents, **4** and **5**, with $R_0$ = $CH(CH_3)C(O)OCH_3$. The combination of $^{1}H$ and $^{13}P$ NMR was crucial to monitor the polymerization and to provide direct information on the reactivity of the CTA. Raft agents **1** and **4** with a phosphorus atom capped with a $BH_3$ moiety provide excellent control with nearly perfect chain-end fidelity for the polymerization of St. For *n*BA polymerization the control is efficient in terms of overall kinetics, control of macromolecular characteristics, and chain-end fidelity. Compounds **3** and **5** are the first examples of P-RAFT agents bearing a free $P^{III}$ Z-group. CTA **3** can be directly used in RAFT polymerization to prepare well-controlled

polystyrenes with a low dispersity of 1.09 – 1.15 with free phosphine ω-chain ends as potential macromolecular ligands. CTAs **3** and **5** do not provide a controlled polymerization of VAc but rather complete inhibition of polymerization because, unlike the $N^{III}$ (dithiocarbamate) analogue, the P atom is reluctant to rehybridize and achieve a planar configuration, as required to engage the lone pair in electronic conjugation with the $CS_2$ unsaturation. Therefore, $P^V$ and $P^{III}$ RAFT agents exhibit similar reactivities, precluding the use of a $P^V$-$P^{III}$ chain-end transformation as a switchable RAFT agent system. Despite the degradation of the macro-RAFT agent obtained from **3** during the *n*BA polymerization, a well-controlled P*n*BA with a reasonably low dispersity around 1.35 could be obtained by an indirect two-step procedure, which involves *n*BA polymerization via the corresponding P-$BH_3$ chain transfer agent, followed by a facile deboranation step. All these chain-end-functionalized polymers may be useful for further applications.

## Experimental Section

### *General*

All reactions were carried out under an argon atmosphere using standard Schlenk techniques. Melting points were determined on the Boetius apparatus and were uncorrected. Solvents were carefully dried by conventional methods and distilled under argon before use. Column chromatography was performed on Carlo Erba silica gel 60, 0.035-0.070 mm. Compounds **1** – **3**[35] and di-*tert*-butylphosphine borane[39] were prepared according to literature procedures. Di-*tert*-butylchlorophosphane (96%, Alfa Aesar), 1,4-diazabicyclo[2.2.2]octane (97%, TCI), *n*-butyllithium (1.6 M solution in hexanes, Sigma Aldrich), and methyl 2-bromopropionate (98%, Sigma Aldrich) were used as received. 2,2'-azobis(2-methylproprionitrile) (AIBN, Sigma-Aldrich, 98%) was recrystallized from methanol and dried at room temperature under vacuum. *n*-butyl acrylate (*n*BA, Sigma-Aldrich, >99%, containing

10-60 ppm monoethyl ether hydroquinone as inhibitor) and styrene (St, Sigma-Aldrich, >99%, containing 4-tert-butylcatechol as a stabilizer) were passed through a column of neutral alumina.

The $^{1}H$, $^{13}C\{^{1}H\}$ and $^{31}P\{^{1}H\}$ NMR spectra were recorded with a Bruker Avance 400 FT-NMR spectrometer. The $^{1}H$ and $^{13}C$ resonances were calibrated relative to the residual solvent peaks and are reported with positive values downfield from TMS. The $^{31}P$ resonances were referenced to 85% $H_3PO_4$ (external standard). For all characterized compounds, the peak assignments in the $^{1}H$ and $^{13}C$ NMR spectra were based on COSY, HSQC and HMBC 2D experiments. HRMS were obtained from dichloromethane solutions with a Xevo G2 Q-TOF spectrometer by the chemical ionization method. Matrix-assisted laser desorption/ionisation – time of flight mass spectrometry (MALDI-TOF-MS) analyses were carried out on Waters MALDI-TOF Micro MX equipped with a nitrogen laser emitting at $\lambda = 357$ nm. All analyses made use of 1,8-dihydroxy-9(10H)-anthracenone (Dithranol) as matrix and $CF_3COONa$ or $CF_3COOAg$ as cationizing agent.

Size-exclusion chromatography (SEC) analyses in THF were carried out on a system composed of an Agilent technologies guard column (PLGel20 μm, 50 × 7.5 mm) and a set of two Waters columns (1 × Styragel® HR 3, 7.8 × 300 mm and 1 × Styragel® HR 4, 7.8 × 300 mm). Detections were conducted using a Wyatt Optilab® rEX refractive index detector and a Varian ProStar 325 UV detector (dual-wavelength analysis). Analyses were carried out at 35°C and a flow rate of 1.0 mL $min^{-1}$. Polystyrene (PSt) standards (580 - 7.5 × $10^5$ g·$mol^{-1}$) for PSt samples and poly(methyl methacrylate) (PMMA) standards (960 – 1.37 × $10^5$ g·$mol^{-1}$) for P*n*BA samples were used for calibration. For the P*n*BA samples, $M_n$ was determined by using the Mark-Houwink-Sakurada parameters of PMMA and P*n*BA.

*Synthesis of* **4**: A solution of di-*tert*-butylphosphine borane, *t*$Bu_2PH{\cdot}BH_3$ (1.00 g, 6.24 mmol) in THF (100 mL) under Ar atmosphere was treated with a slight excess of *n*-butyllithium (4.1 mL, 1.6 M in hexane) at -40°C. The resulting bright yellow mixture was allowed to warm up to 0°C and stirred for 1 h. Then a large excess of $CS_2$ (2.2 mL, 33.6 mmol) was added dropwise at 0°C to yield a dark red solution. The reaction vessel was covered with aluminum foil and was allowed to warm up to 12°C and stirred for 15 min. Methyl 2-bromopropionate (1.10 mL, 9.87 mmol) was then added, and the dark red solution was stirred for an additional 4 h at 12–13°C. After removal of the solvent under reduced pressure, the residual product was subjected to column chromatography (silica gel, hexane/toluene (1:1 v/v)). Removal of the solvent resulted in 1.025 g (51% yield) of the product as a pink amorphous solid.

**MP** = 62-64°C. **$^1$H NMR (400MHz, $CDCl_3$) δ (ppm):** 4.61 (1H, qd, $^3J_{HH}$ = 7.4Hz, $^4J_{HP}$ = 1.5Hz, C*H*$CH_3$), 3.72 (3H, s, OC*H*$_3$), 1.62 (3H, dd, $^3J_{HH}$ = 7.4Hz, $^4J_{HP}$ = 1.0Hz, CHC*H*$_3$), 1.43 (9H, d, $^3J_{HP}$ = 1.4Hz, C(C*H*$_3$)$_3$), 1.40 (9H, d, $^3J_{HP}$ = 1.4Hz, C(C*H*$_3$)$_3$)), 0.50-1.50 (3H, br q, B*H*$_3$). **$^{13}$C{$^1$H} (125MHz, $CDCl_3$) δ (ppm):** 231.9 (d, $^1J_{CP}$ = 10.9Hz, *C*(S)S), 170.6 (*C*(O)O), 52.8 (O*C*$H_3$), 47.6 (d, $^3J_{CP}$ = 1.7 Hz, *C*H$CH_3$), 35.8 (d, $^1J_{CP}$ = 20.6 Hz, *C*$(CH_3)_3$), 35.7 (d, $^1J_{CP}$ = 20.2 Hz, *C*$(CH_3)_3$), 28.5 (d, $^2J_{CP}$ = 1.6 Hz, C(*C*$H_3$)$_3$), 28.4 (d, $^2J_{CP}$ = 1.8Hz, C(*C*$H_3$)$_3$), 15.3 (CH*C*$H_3$). **$^{11}$B{$^1$H} (128 MHz, $CDCl_3$) δ (ppm):** -41.1 (br d). **$^{31}$P{$^1$H} (162MHz, $CDCl_3$) δ (ppm):** 68.9 (br d). **HRMS (DCI, $CH_4$):** 321.1281 (100%, 321.1283 for $C_{13}H_{27}BO_2PS_2$: M-H) (Figures S51 – S54).

*Synthesis of* **5**: A solution of the carbodithioate **7** (0.474 g, 1.47 mmol) in toluene (30 mL), under Ar atmosphere in a Schlenk tube covered with aluminum foil, was treated with DABCO (0.357 g, 2.92 mmol). The reaction mixture was stirred for 6 h at 60°C. After removal of the solvent under reduced pressure, the residual product was subjected to column

chromatography (silica gel, hexane/toluene (1:1 v/v)). Removal of the solvent resulted in 0.430 g (95% yield) of the product as a pink oil.

**$^{1}$H (400MHz, $CDCl_3$) δ (ppm):** 4.76 (1H, q of d, $^{3}J_{HH}$ = 7.3Hz, $^{4}J_{HP}$ = 3.3Hz, C*H*$CH_3$), 3.72 (1H, s, OC*H*$_3$), 1.56 (1H, dd, $^{3}J_{HH}$ = 7.4Hz, $^{5}J_{HP}$ = 1.6Hz, CHC*H*$_3$), 1.298 (9H, d, $^{3}J_{HP}$ = 12.4Hz, C(C*H*$_3$)$_3$), 1.293 (9H, d, $^{3}J_{HP}$ = 12.4Hz, C(C*H*$_3$)$_3$). **$^{13}$C (125MHz, $CDCl_3$) δ (ppm):** 247.3 (d, $^{1}J_{CP}$ = 60.8Hz, *C*(S)S), 171.4 (*C*(O)O), 52.6 (O*C*$H_3$), 47.1 (d, $^{3}J_{CP}$ = 19.6Hz, *C*HCH$_3$), 35.1 (d, $^{1}J_{CP}$ = 27.0Hz, *C*(CH$_3$)$_3$), 35.0 (d, $^{1}J_{CP}$ = 27.1Hz, *C*(CH$_3$)$_3$), 29.82 (d, $^{2}J_{CP}$ = 13.9Hz, C(*C*H$_3$)$_3$), 29.79 (d, $^{2}J_{CP}$ = 14.0Hz, C(*C*H$_3$)$_3$), 15.6 (CH*C*H$_3$). **$^{31}$P{$^{1}$H} (162MHz, $CDCl_3$) δ (ppm):** 66.9. **HRMS (DCI, $CH_4$):** 309.1091 (50%, 309.1106 for $C_{13}H_{26}O_2PS_2$: M+H) (Figures S55 – S57).

*St and nBA polymerization procedure*

A solution containing the monomer (4.10 g for *n*BA, 3.34 g for St), the RAFT agent (1.1 × $10^{-4}$ mol) and AIBN (1.8 mg, 1.1 × $10^{-5}$ mol) in toluene (1.42 g for *n*BA, 2.02 g for St) was prepared in a 15 mL tube. Further, the solution was transferred into 6 sealing tubes, degassed by three freeze–pump–thaw cycles and sealed under vacuum. The tubes were heated at 60°C in a thermostated heating block. At the desired time, each polymerization was quenched by freezing in liquid nitrogen and the obtained solution was analyzed by NMR to estimate the monomer conversion. Then the excess amounts of monomer and solvent were removed by evaporation at ambient temperature under vacuum and the residues were analyzed using SEC.

*VAc polymerization procedure*

The solution that contained the monomer (2.76 g), RAFT agent (1.1 × $10^{-4}$ mol) and AIBN (3.6 mg, 2.2 × $10^{-5}$ mol) in EtOAc (2.76 g) or without solvent was prepared in a 15 mL tube. Further, the solution was transferred into sealing tubes, degassed by three freeze–pump–

thaw cycles and sealed under vacuum. The tubes were heated at 70°C in a thermostated heating block for the requisite times. The polymerization was quenched by freezing in liquid nitrogen and the obtained solution was analyzed with NMR to estimate monomer conversion. Then the excess amounts of monomer and solvent were removed by evaporation at ambient temperature under vacuum and the residues were analyzed using SEC.

*Procedure for the kinetic measurements*

A solution containing the monomer (2.78 g, 0.027 mol), the RAFT agent ($8.9 \times 10^{-5}$ mol), AIBN (1.5 mg, $8.9 \times 10^{-5}$ mol), 1,4-dioxane (0.078 g, $8.9 \times 10^{-4}$ mol) and triphenylphosphine sulfide (0.025 g, $8.9 \times 10^{-5}$ mol) in $C_6D_6$ (1.76 g, 0.021 mol) was prepared in a 15 mL Schlenk tube with a PTFE needle valve and degassed by three freeze–pump–thaw cycles. This solution was then transferred into 8 NMR tubes in the glove box under an argon atmosphere and sealed with rubber septa. The tubes were heated at 60 °C in a thermostated heating block. At the desired time, each tube was quenched by freezing in liquid nitrogen and the obtained solution was analyzed by NMR. Then the excess amounts of monomer and solvent were removed by evaporation at ambient temperature under vacuum and the residues were analyzed using SEC.

*Procedure for the preparation of PSt-**1**, PnBA-**4***

The solution (5 mL) that contained the monomer (3.33 g, 0.032 mol for St; 4.10 g, 0.032 mol for *n*BA), RAFT agent ($1.1 \times 10^{-4}$ mol), AIBN ($1.1 \times 10^{-4}$ mol), in toluene (1.42 mL for *n*BA, 2.10 mL for St) was prepared in a 15 mL Schlenk tube with a PTFE needle valve and degassed by three freeze–pump–thaw cycles. Then the solution was heated at 60°C in a thermostated heating block for the requisite times (24 h for PSt-**1**, 10 h for P*n*BA-**1**). The polymerization was quenched by freezing in liquid nitrogen and the obtained solution was

analyzed with NMR. Then the excess amounts of monomer and solvent were removed by evaporation at ambient temperature under vacuum and the residues were dissolved in $CHCl_3$ and precipitated by cold $CH_3OH$. Obtained solids (pink PSt-**1** and P*n*BA-**4**) were dried under vacuum and analyzed using SEC.

*Polymer ω-chain ends deboranation*

A solution of the desired polymer (0.2 g of PSt-**1** or PnBA-**4**) in THF (10 mL) was prepared in a 15 mL Schlenk tube with a PTFE needle valve and degassed by three freeze–pump–thaw cycles. Degassed $Et_3N$ (0.05 mL) was added dropwise under Ar. The resulting mixtures were stirred for 24 h at ambient temperature. All volatiles were then removed by evaporation at ambient temperature under vacuum. The obtained pink solids (PSt-**1** (-$BH_3$) and P*n*BA-**4** (-$BH_3$)) were dried under vacuum and analyzed using $^{31}P$ NMR and SEC.

*Computational details*

The computational work was carried out with the Gaussian09 suite of programs.[40] Gas-phase geometry optimizations were executed without any symmetry constraint using the M06-2X functional[41] and the 6-31G(d,p) basis set for all atoms. All final geometries were characterized as stationary points by verifying that all second derivatives of the energy were positive. Thermochemical corrections were obtained at 298.15 K on the basis of frequency calculations, using the standard ideal gas, rigid rotor and harmonic oscillator approximations. A further correction of 1.95 Kcal/mol was applied to bring the G values from the gas phase (1 atm) to the solution (1 mol/L) standard state.[42]

**Acknowledgements**

We thank the Agence Nationale de la Recherche for support of this work through grant ANR-16-CE29-0014-RAFTSWITCH. Additional support from the CNRS (Centre National de la Recherche Scientifique) is also gratefully acknowledged. We also thank the CALMIP mesocenter of the University of Toulouse for the allocation of computational resources. The authors thank Dr. Ihor Kulai for fruitful discussions.

**Associated content:**

The Supporting Information is available free of charge on the ACS Publications website at DOI: . Tables S1−S3 and Figures S1−S32 ($^{1}$H and $^{31}$P NMR, SEC-RI chromatograms).

**References:**

(1) Moad, G.; Rizzardo, E.; Thang, S. H. Living Radical Polymerization by the RAFT Process – A Third Update. *Aust. J. Chem.* **2012**, *65* (8), 985. https://doi.org/10.1071/CH12295.

(2) Perrier, S. 50th Anniversary Perspective: RAFT Polymerization—A User Guide. *Macromolecules* **2017**, *50* (19), 7433–7447. https://doi.org/10.1021/acs.macromol.7b00767.

(3) Chiefari, J.; Mayadunne, R. T. A.; Moad, C. L.; Moad, G.; Rizzardo, E.; Postma, A.; Thang, S. H. Thiocarbonylthio Compounds (SC(Z)S−R) in Free Radical Polymerization with Reversible Addition-Fragmentation Chain Transfer (RAFT Polymerization). Effect of the Activating Group Z. *Macromolecules* **2003**, *36* (7), 2273–2283. https://doi.org/10.1021/ma020883+.

(4) Destarac, M.; Charmot, D.; Franck, X.; Zard, S. Z. Dithiocarbamates as Universal Reversible Addition-Fragmentation Chain Transfer Agents. *Macromol. Rapid Commun.*

**2000**, *21* (15), 1035–1039. https://doi.org/10.1002/1521-3927(20001001)21:15<1035::AID-MARC1035>3.0.CO;2-5.

(5) Chong, ) Y. K.; Krstina, J.; Le, T. P. T.; Moad, G.; Postma, A.; Rizzardo, E.; Thang, S. H. Thiocarbonylthio Compounds [SC(Ph)S−R] in Free Radical Polymerization with Reversible Addition-Fragmentation Chain Transfer (RAFT Polymerization). Role of the Free-Radical Leaving Group (R). *Macromolecules* **2003**, *36* (7), 2256–2272. https://doi.org/10.1021/ma020882h.

(6) Keddie, D. J.; Moad, G.; Rizzardo, E.; Thang, S. H. RAFT Agent Design and Synthesis. *Macromolecules* **2012**, *45* (13), 5321–5342. https://doi.org/10.1021/ma300410v.

(7) Destarac, M. On the Critical Role of RAFT Agent Design in Reversible Addition-Fragmentation Chain Transfer (RAFT) Polymerization. *Polym. Rev.* **2011**, *51* (2), 163–187. https://doi.org/10.1080/15583724.2011.568130.

(8) Chiefari, J.; Chong, Y. K. (Bill); Ercole, F.; Krstina, J.; Jeffery, J.; Le, T. P. T.; Mayadunne, R. T. A.; Meijs, G. F.; Moad, C. L.; Moad, G.; Rizzardo, E.; Thang, S. H. Living Free-Radical Polymerization by Reversible Addition−Fragmentation Chain Transfer: The RAFT Process. *Macromolecules* **1998**, *31* (16), 5559–5562. https://doi.org/10.1021/ma9804951.

(9) Moad, G. Mechanism and Kinetics of Dithiobenzoate-Mediated RAFT Polymerization – Status of the Dilemma. *Macromol. Chem. Phys.* **2014**, *215* (1), 9–26. https://doi.org/10.1002/macp.201300562.

(10) Mayadunne, R. T. A.; Rizzardo, E.; Chiefari, J.; Chong, Y. K.; Moad, G.; Thang, S. H. Living Radical Polymerization with Reversible Addition−Fragmentation Chain Transfer (RAFT Polymerization) Using Dithiocarbamates as Chain Transfer Agents. *Macromolecules* **1999**, *32* (21), 6977–6980. https://doi.org/10.1021/ma9906837.

(11) Destarac, M.; Charmot, D.; Franck, X.; Zard, S. Z. Dithiocarbamates as Universal Reversible Addition-Fragmentation Chain Transfer Agents. *Macromol. Rapid Commun.* **2000**, *21* (15), 1035–1039. https://doi.org/10.1002/1521-3927(20001001)21:15<1035::AID-MARC1035>3.0.CO;2-5.

(12) Destarac, M.; Bzducha, W.; Taton, D.; Gauthier-Gillaizeau, I.; Zard, S. Z. Xanthates as Chain-Transfer Agents in Controlled Radical Polymerization (MADIX): Structural Effect of the O-Alkyl Group. *Macromol. Rapid Commun.* **2002**, *23* (17), 1049–1054. https://doi.org/10.1002/marc.200290002.

(13) Fuchs, A. V.; Thurecht, K. J. Stability of Trithiocarbonate RAFT Agents Containing Both a Cyano and a Carboxylic Acid Functional Group. *ACS Macro Lett.* **2017**, *6* (3), 287–291. https://doi.org/10.1021/acsmacrolett.7b00100.

(14) Benaglia, M.; Chiefari, J.; Chong, Y. K.; Moad, G.; Rizzardo, E.; Thang, S. H. Universal (Switchable) RAFT Agents. *J. Am. Chem. Soc.* **2009**, *131* (20), 6914–6915. https://doi.org/10.1021/ja901955n.

(15) Keddie, D. J.; Guerrero-Sanchez, C.; Moad, G.; Rizzardo, E.; Thang, S. H. Switchable Reversible Addition–Fragmentation Chain Transfer (RAFT) Polymerization in Aqueous Solution, N,N-Dimethylacrylamide. *Macromolecules* **2011**, *44* (17), 6738–6745. https://doi.org/10.1021/ma200760q.

(16) Moad, G.; Keddie, D.; Guerrero-Sanchez, C.; Rizzardo, E.; Thang, S. H. Advances in Switchable RAFT Polymerization. *Macromol. Symp.* **2015**, *350* (1), 34–42. https://doi.org/10.1002/masy.201400022.

(17) Destarac, M.; Matioszek, D.; Vila, X.; Ruchmann-Sternchuss, J.; Zard, S. Z. How Can Xanthates Control the RAFT Polymerization of Methacrylates? In *Reversible Deactivation Radical Polymerization: Mechanisms and Synthetic Methodologies*; ACS

Symposium Series; American Chemical Society, 2018; Vol. 1284, pp 291–305. https://doi.org/10.1021/bk-2018-1284.ch013.

(18) Destarac, M.; Taton, D.; Zard, S. Z.; Saleh, T.; Six, Y. On the Importance of Xanthate Substituents in the MADIX Process. In *Advances in Controlled/Living Radical Polymerization*; ACS Symposium Series; American Chemical Society, 2003; Vol. 854, pp 536–550. https://doi.org/10.1021/bk-2003-0854.ch037.

(19) Gardiner, J.; Martinez-Botella, I.; Tsanaktsidis, J.; Moad, G. Dithiocarbamate RAFT Agents with Broad Applicability – the 3,5-Dimethyl-1H-Pyrazole-1-Carbodithioates. *Polym. Chem.* **2015**, *7* (2), 481–492. https://doi.org/10.1039/C5PY01382H.

(20) Gardiner, J.; Martinez-Botella, I.; Kohl, T. M.; Krstina, J.; Moad, G.; Tyrell, J. H.; Coote, M. L.; Tsanaktsidis, J. 4-Halogeno-3,5-Dimethyl-1H-Pyrazole-1-Carbodithioates: Versatile Reversible Addition Fragmentation Chain Transfer Agents with Broad Applicability. *Polym. Int.* **2017**, *66* (11), 1438–1447. https://doi.org/10.1002/pi.5423.

(21) Theis, A.; Stenzel, M. H.; Davis, T. P.; Coote, M. L.; Barner-Kowollik, C. A Synthetic Approach to a Novel Class of Fluorine-Bearing Reversible Addition-Fragmentation Chain Transfer (RAFT) Agents: F-RAFT. In *Aust. J. Chem.*; CSIRO PUBLISHING, 2005; Vol. 58, pp 437–441. https://doi.org/10.1071/CH05069.

(22) Matioszek, D.; Brusylovets, O.; James Wilson, D.; Mazières, S.; Destarac, M. Reversible Addition-Fragmentation Chain-Transfer Polymerization of Vinyl Monomers with N,N-Dimethyldiselenocarbamates. *J. Polym. Sci. A Polym. Chem.* **2013**, *51* (20), 4361–4368. https://doi.org/10.1002/pola.26850.

(23) Demirci, S.; Kinali-Demirci, S.; Caykara, T. A New Selenium-Based RAFT Agent for Surface-Initiated RAFT Polymerization of 4-Vinylpyridine. *Polymer* **2013**, *54* (20), 5345–5350. https://doi.org/10.1016/J.POLYMER.2013.07.060.

(24) Zeng, J.; Zhang, Z.; Zhu, J.; Zhou, N.; Cheng, Z.; Zhu, X. Selenium-Substituted Carbonates as Mediators for Controlled Radical Polymerization. *J. Polym. Sci. A Polym. Chem.* **2013**, *51* (12), 2606–2613. https://doi.org/10.1002/pola.26648.

(25) Kulai, I.; Saffon-Merceron, N.; Voitenko, Z.; Mazières, S.; Destarac, M. Alkyl Triarylstannanecarbodithioates: Synthesis, Crystal Structures, and Efficiency in RAFT Polymerization. *Chem. Eur. J.* **2017**, *23* (63), 16066–16077. https://doi.org/10.1002/chem.201703412.

(26) Kulai, I.; Brusylovets, O.; Voitenko, Z.; Harrisson, S.; Mazières, S.; Destarac, M. RAFT Polymerization with Triphenylstannylcarbodithioates (Sn-RAFT). *ACS Macro Letters* **2015**, *4* (8), 809–813. https://doi.org/10.1021/acsmacrolett.5b00329.

(27) Laus, M.; Papa, R.; Sparnacci, K.; Alberti, A.; Benaglia, M.; Macciantelli, D. Controlled Radical Polymerization of Styrene with Phosphoryl- and (Thiophosphoryl)Dithioformates as RAFT Agents. *Macromolecules* **2001**, *34* (21), 7269–7275. https://doi.org/10.1021/ma010299l.

(28) Alberti, A.; Benaglia, M.; Laus, M.; Macciantelli, D.; Sparnacci, K. Direct ESR Detection of Free Radicals in the RAFT Polymerization of Styrene. *Macromolecules* **2003**, *36* (3), 736–740. https://doi.org/10.1021/ma025713b.

(29) Mazières, S.; Kulai, I.; Geagea, R.; Ladeira, S.; Destarac, M. Phosphinoyl and Thiophosphinoylcarbodithioates: Synthesis, Molecular Structure, and Application as New Efficient Mediators for RAFT Polymerization. *Chem. Eur. J.* **2015**, *21* (4), 1726–1734. https://doi.org/10.1002/chem.201404631.

(30) Geagea, R.; Ladeira, S.; Mazières, S.; Destarac, M. Chromium and Molybdenum Pentacarbonyl Complexes of Phosphinocarbodithioates: Synthesis, Molecular Structure and Behaviour in RAFT Polymerisation. *Chem. Eur. J.* **2011**, *17* (13), 3718–3725. https://doi.org/10.1002/chem.201002342.

(31) Kulai, I.; Karpus, A.; Soroka, L.; Valyaev, D. A.; Bourdon, V.; Manoury, E.; Poli, R.; Destarac, M.; Mazières, S. Manganese Phosphinocarbodithioate for RAFT Polymerisation with Sunlight-Induced Chain End Post-Treatment. *Polym. Chem.* **2018**. https://doi.org/10.1039/C8PY01279B.

(32) Kulai, I.; Voitenko, Z.; Mazières, S.; Destarac, M. Enhanced Control of Phosphinoylcarbodithioate-Mediated RAFT Polymerization: Key Role of Substituents at the Phosphorus Center. *Macromolecules* **2019**. https://doi.org/10.1021/acs.macromol.9b01642.

(33) Glassner, M.; Delaittre, G.; Kaupp, M.; Blinco, J. P.; Barner-Kowollik, C. (Ultra)Fast Catalyst-Free Macromolecular Conjugation in Aqueous Environment at Ambient Temperature. *J. Am. Chem. Soc.* **2012**, *134* (17), 7274–7277. https://doi.org/10.1021/ja301762y.

(34) Skaff, H.; Emrick, T. Reversible Addition Fragmentation Chain Transfer (RAFT) Polymerization from Unprotected Cadmium Selenide Nanoparticles. *Angew. Chem. Int. Ed.* **2004**, *43* (40), 5383–5386. https://doi.org/10.1002/anie.200453822.

(35) Karpus, A.; Daran, J.-C.; Poli, R.; Mazières, S.; Destarac, M. A.; Manoury, E. Synthesis of S -Alkyl Phosphinocarbodithioates with Switch between P(III) and P(V) Derivatives. *J. Org. Chem.* **2019**, *84* (15), 9446–9453. https://doi.org/10.1021/acs.joc.9b00590.

(36) Benaglia, M.; Chen, M.; Chong, Y. K.; Moad, G.; Rizzardo, E.; Thang, S. H. Polystyrene-Block-Poly(Vinyl Acetate) through the Use of a Switchable RAFT Agent. *Macromolecules* **2009**, *42* (24), 9384–9386. https://doi.org/10.1021/ma9021086.

(37) Girard, E.; Tassaing, T.; Marty, J.-D.; Destarac, M. Influence of Macromolecular Characteristics of RAFT/MADIX Poly(Vinyl Acetate)-Based (Co)Polymers on Their Solubility in Supercritical Carbon Dioxide. *Polym. Chem.* **2011**, *2* (10), 2222–2230. https://doi.org/10.1039/C1PY00209K.

(38) Moad, G. A Critical Survey of Dithiocarbamate Reversible Addition-Fragmentation Chain Transfer (RAFT) Agents in Radical Polymerization. *J. Polym. Sci. A Polym. Chem.* **2019**, *57* (3), 216–227. https://doi.org/10.1002/pola.29199.

(39) Frew, J. J. R.; Damian, K.; Van Rensburg, H.; Slawin, A. M. Z.; Tooze, Robert. P.; Clarke, M. L. Palladium(II) Complexes of New Bulky Bidentate Phosphanes: Active and Highly Regioselective Catalysts for the Hydroxycarbonylation of Styrene. *Chem. Eur. J.* **2009**, *15* (40), 10504–10513. https://doi.org/10.1002/chem.200901178.

(40) Frisch, M. J.; Trucks, G. W.; Schlegel, H. B.; Scuseria, G. E.; Robb, M. A.; Cheeseman, J. R.; Scalmani, G.; Barone, V.; Mennucci, B.; Petersson, G. A.; Nakatsuji, H.; Caricato, M.; Li, X.; Hratchian, H. P.; Izmaylov, A. F.; Bloino, J.; Zheng, G.; Sonnenberg, J. L.; Hada, M.; Ehara, M.; Toyota, K.; Fukuda, R.; Hasegawa, J.; Ishida, M.; Nakajima, T.; Honda, Y.; Kitao, O.; Nakai, H.; Vreven, T.; Montgomery, J. A., Jr.; Peralta, J. E.; Ogliaro, F.; Bearpark, M.; Heyd, J. J.; Brothers, E.; Kudin, K. N.; Staroverov, V. N.; Kobayashi, R.; Normand, J.; Raghavachari, K.; Rendell, A.; Burant, J. C.; Iyengar, S. S.; Tomasi, J.; Cossi, M.; Rega, N.; Millam, J. M.; Klene, M.; Knox, J. E.; Cross, J. B.; Bakken, V.; Adamo, C.; Jaramillo, J.; Gomperts, R.; Stratmann, R. E.; Yazyev, O.; Austin, A. J.; Cammi, R.; Pomelli, C.; Ochterski, J. W.; Martin, R. L.; Morokuma, K.; Zakrzewski, V. G.; Voth, G. A.; Salvador, P.; Dannenberg, J. J.; Dapprich, S.; Daniels, A. D.; Farkas, Ö.; Foresman, J. B.; Ortiz, J. V.; Cioslowski, J.; Fox, D. J. *Gaussian 09 Revision D.01*; Gaussian, Inc.: Wallingford CT, 2009.

(41) Zhao, Y.; Truhlar, D. G. The M06 Suite of Density Functionals for Main Group Thermochemistry, Thermochemical Kinetics, Noncovalent Interactions, Excited States, and Transition Elements: Two New Functionals and Systematic Testing of Four M06-Class Functionals and 12 Other Functionals. *Theor. Chem. Acc.* **2008**, *120* (1), 215–241. https://doi.org/10.1007/s00214-007-0310-x.

(42) Bryantsev, V. S.; Diallo, M. S.; Goddard III, W. A. Calculation of Solvation Free Energies of Charged Solutes Using Mixed Cluster/Continuum Models. *J. Phys. Chem. B* **2008**, *112* (32), 9709–9719. https://doi.org/10.1021/jp802665d.